Renal Sensory Nerves Increase Sympathetic Nerve Activity and Blood Pressure in 2-Kidney 1-Clip Hypertensive Mice

by

Jason Ong

Bachelor of Philosophy, University of Pittsburgh, 2020

Submitted to the Graduate Faculty of the

Dietrich School of Arts and Sciences & University Honors College in partial fulfillment

of the requirements for the degree of

Bachelor of Philosophy

University of Pittsburgh

2020

UNIVERSITY OF PITTSBURGH

DIETRICH SCHOOL OF ARTS AND SCIENCES &
UNIVERSITY HONORS COLLEGE

This thesis was presented

by

Jason Ong

It was defended on

February 13, 2020

and approved by

Susan R. Sesack Ph.D., Department of Neuroscience

Alan Sved, Ph.D., Department of Neuroscience

Gregory Fink, Ph.D., Department of Pharmacology and Toxicology, Michigan State University

Thesis Advisor/Dissertation Director: Sean Stocker, Ph.D., Department of Medicine, Division of Renal Electrolyte

Renal Sensory Nerves Increase Sympathetic Nerve Activity and Blood Pressure in 2-Kidney 1-Clip Hypertensive Mice

Jason Ong, BPhil

University of Pittsburgh, 2020

Renal denervation lowers arterial blood pressure (ABP) in multiple clinical trials and some experimental models of hypertension. These antihypertensive effects have been attributed to the removal of renal afferent nerves. The purpose of the present study was to define the function, anatomy, and contribution of mouse renal sensory neurons to a renal-nerve dependent model of hypertension. First, electrical stimulation of mouse renal afferent nerves produced frequency-dependent increases in ABP that were eliminated by ganglionic blockade. Stimulus-triggered averaging revealed renal afferent stimulation significantly increased splanchnic, renal, and lumbar sympathetic nerve activity (SNA). Second, kidney injection of wheat germ agglutinin into male C57Bl6 mice (12-14 weeks, Jackson Laboratories) produced ipsilateral labeling in the T11-L2 dorsal root ganglia. Next, 2K1C hypertension was produced in male C57Bl6 mice (12-14 weeks, Jackson Laboratories) by placement of a 0.5mm length of PTFE tubing around the left renal artery. 2K1C mice displayed an elevated ABP measured via telemetry and greater fall in mean ABP to ganglionic blockade at day 14 or 21 vs day 0. Renal afferent discharge was significantly higher in 2K1C-clipped versus 2K1C-unclipped or sham kidneys. In addition, 2K1C-clipped versus 2K1C-unclipped or sham kidneys had lower renal mass and higher mRNA levels of several pro-inflammatory cytokines. Finally, both ipsilateral renal denervation (10% phenol) or selective denervation of renal afferent nerves (periaxonal application of 33 mM capsaicin) at time of

clipping resulted in lower ABP of 2K1C mice at Days 14 or 21. These findings suggest mouse renal sensory neurons are activated to increase SNA and ABP in 2K1C hypertension.

Table of Contents

List of Tables

List of Figures

Preface

A version of this thesis was published in the Journal of Neurophysiology with the included authors, except for a couple of paragraphs in the introduction.

Jason Ong[1,2], Brian J. Kinsman[1], Alan F. Sved[2], Brittany M. Rush[1], Roderick J. Tan[1], Marcelo D. Carattino[1], and Sean D. Stocker[1]

[1]Department of Medicine, Division of Renal-Electrolyte

[2]Department of Neuroscience

University of Pittsburgh, Pittsburgh, PA.

1.0 Introduction

Renal denervation lowers arterial blood pressure (ABP) in several experimental models of hypertension including the Spontaneously Hypertensive Rat, Deoxycorticosterone-Salt Model, and 2-Kidney-1-Clip (2K1C) (DiBona and Kopp 1997, Osborn and Foss 2017). In addition, the majority of clinical trials report renal denervation lowered ABP in humans (Symplicity HTN-1, Symplicity HTN-2, DENERHTN, and SPYRAL) (Krum, Schlaich et al. 2009, Krum, Schlaich et al. 2014, Azizi, Sapoval et al. 2015, Townsend, Mahfoud et al. 2017). The therapeutic effects of renal denervation have been attributed to the removal of sympathetic efferent and/or afferent fibers (Osborn and Banek 2018).

Renal efferent or sympathetic nerves originate in the intermediolateral cell column of the spinal cord from T6-L2, synapse in the paravertebral chain ganglia and prevertebral ganglia and project down along the renal artery and vein. These nerves innervate renal arterioles, juxtaglomerular cells, and the entire renal tubular system (Osborn and Foss 2017). A number of studies indicate that activation of renal efferent fibers increases renin secretion and promotes tubular sodium reabsorption (Osborn and Foss 2017). In regard to the therapeutic effects of renal denervation, renal denervation in humans lowered total peripheral resistance without changes in cardiac output (Ewen, Cremers et al. 2015). Additionally, renal denervation lowered the renal resistivity index without changes in glomerular filtration rate or urinary albumin excretion (Mahfoud, Cremers et al. 2012).

The second class of renal nerves are afferent or sensory nerves. Immunohistochemical staining of sensory nerves with calcitonin gene-related peptide reveal these nerves directly innervate the pelvic wall and to a lesser extent the renal vasculature. Sensory nerve fibers project

centrally through T6 and L4 DRG, with the majority in T12-T13. These nerves synapse in the ipsilateral dorsal horn of Laminae I, III and IV of the spinal cord, onto interneurons of the central nervous system that project to areas associated with cardiovascular regulation, such as the rostral ventrolateral medulla. Some renal sensory nerves may also project directly to the brainstem (Kopp 2015). Stimulation of renal afferent fibers in rats and cats increased ABP (Stella, Golin et al. 1984, Caverson and Ciriello 1987, Stella, Weaver et al. 1987, Simon, Kasting et al. 1989). Direct recording of renal afferent activity indicates these fibers respond to mechanical and chemical stimuli (Recordati, Moss et al. 1978, Recordati, Moss et al. 1980, Recordati, Moss et al. 1981). Increased renal pelvic pressure as low as 3 mmHg activates renal sensory nerves. In addition, there are two groups of chemosensitive renal sensory nerves. R1 receptors are not spontaneously active but increase in firing rate under renal ischemia induced by renal artery occlusion. R2 receptors have a basal firing rate which increases to changes in pelvic urine composition, including high NaCl concentration (3-5%) and mannitol (1M) (Recordati, Moss et al. 1978, Recordati, Moss et al. 1980, Recordati, Moss et al. 1981).

In regards to the contribution of renal afferents on the antihypertensive effects of renal denervation, dorsal rhizotomy to surgically remove all types of sensory fibers across multiple levels of the spinal cord and end-organs lowered ABP in some experimental models of hypertension (Wyss, Aboukarsh et al. 1986, Campese and Kogosov 1995). In addition, renal denervation in humans decreased muscle sympathetic nerve activity (SNA) (Hering, Lambert et al. 2013, Hering, Marusic et al. 2014, Grassi, Seravalle et al. 2015), reduced resting plasma glucose (Witkowski, Prejbisz et al. 2011), and reduced cardiac arrhythmias (Linz, Hohl et al. 2018). Recently, periaxonal application of capsaicin to selectively ablate renal sensory fibers reduced ABP in deoxycorticosterone-salt rat (Banek, Knuepfer et al. 2016) but not in the Dahl-salt-

sensitive rat (Foss, Fink et al. 2016), angiotensin II-salt rat (Foss, Fiege et al. 2018), and angiotensin II-infused mouse (Xiao, Kirabo et al. 2015) models of hypertension. Altogether, these observations suggest that the antihypertensive effects of renal denervation may be partly attributed to removal of renal afferent nerves in certain models of hypertension.

The majority of data regarding renal sensory nerves originates from studies performed in rats or larger animal models. Although mice currently represent the most common biomedical research model and transgenic lines provide a platform to address unique research questions, no information is currently available of mouse renal sensory nerves regarding the function, anatomical location of cell bodies, and contribution to neurogenic hypertension. Therefore, the purpose of the present study was to lay a foundational framework of mouse renal sensory nerves and then test the contribution of these nerves in an established renal nerve-dependent model of hypertension. The current study utilized an array of approaches including renal afferent nerve stimulation and simultaneous sympathetic nerve recordings, neuronal anatomical tracing, direct renal afferent nerve recording, and total versus selective afferent renal nerve denervation in a renovascular of 2K1C model of hypertension.

Renovascular hypertension produced by renal stenosis is the primary cause of secondary hypertension, accounting for 2-5% of systemic hypertension (de Mast Q 2009). Experimentally, renal stenosis is produced by placement of a fixed diameter cuff around the renal artery. The initial hypertension is mediated by the renin-angiotensin-aldosterone system, as administration of angiotensin converting enzyme inhibitors or angiotensin receptor blockers attenuates/blocks the increased blood pressure (Romero et al. 1977). Chronically, blockade of the RAAS does not lower blood pressure to the same extent, suggesting other mechanisms. At this stage, this elevated ABP may be neurogenically mediated given a greater drop to ganglionic blockade. Furthermore, renal

denervation has been shown to lower ABP in several models of hypertension. However, there are limited data to directly assess the anti-hypertensive effect of renal denervation (whether efferent or afferent) in this cohort (Krum, Schlaich et al. 2009, Krum, Schlaich et al. 2014, Azizi, Sapoval et al. 2015, Townsend, Mahfoud et al. 2017).

2.0 Methods

All of the experimental procedures conform to the National Institutes of Health Guide for the Care and Use of Laboratory Animals and were approved by the Institutional Animal Care and Use Committee at the University of Pittsburgh School of Medicine. Male C57Bl6J mice (8-12 weeks of age, strain 00664, Jackson Laboratories) were housed in a temperature-controlled room (22±1˚C), fed 0.1% NaCl chow (D17020, Research Diets), and given access to deionized water.

2.1 Experiment 1

Experiment 1 investigated whether activation of mouse renal sensory nerves increases SNA and ABP. Mice (n=6) were anesthetized with isoflurane and instrumented with femoral arterial and venous catheters. Body temperature was maintained at 37.0±0.2˚C through a servo-controlled temperature controller and rectal probe (CWE, Inc). Through a retroperitoneal incision, the right renal nerve was isolated, placed on bipolar stainless-steel electrodes, cut distal, and insulated with KWIK-SIL. After the mouse stabilized for >10 min at 1.8% isoflurane, the renal afferent nerves were stimulated electrically (1ms pulse, 10s train, 200uA) at various frequencies (2, 5, 10, 20, 30, 50 Hz) in a random order separated by 5 min. To test the contribution of the sympathetic nervous system, the stimulation was repeated after administration of the ganglionic blocker chlorisondamine (5mg/kg, IV). The contribution of vasopressin was tested in a half of the animals by administration of [β-Mercapto-β,β-cycloptenamethyleneproionyl1,O-me-Tyr2,Arg8]-vasopressin (10ug/kg, IV) prior to chlorisondamine. In a second set of mice anesthetized with

isoflurane (n=4), the left splanchnic, renal, and lumbar sympathetic nerves were isolated, placed on bipolar stainless-steel electrodes, and insulated with KWIK-SIL. Signals were filtered (100-1000 Hz), digitized (2 kHz), rectified, and integrated (10ms time constant) using a Micro1401 and Spike2 software (Cambridge Electronic Design). Due to electrical artifacts produced by electrical stimulation of the renal afferent nerves, stimulus-triggered averaging was performed before and after a single electrical pulse was applied to the renal afferent nerve (1ms duration, 30 sweeps, 100uA). To evaluate whether the type of anesthesia impacted these cardiovascular responses, renal afferent stimulation was repeated in mice (n=3) anesthetized with urethane (1.2mg/kg body weight, IV) after induction with isoflurane.

2.2 Experiment 2

Experiment 2 identified the location of renal sensory neurons. Mice (n=4) were anesthetized with isoflurane. After a midline laparotomy to visualize the kidneys, a glass micropipette (OD: 20-40µm) containing Wheat-Germ-Agglutinin (WGA tagged with Alexa Fluor 488 or 594, 10%) was lowered into the kidneys using coordinates relative to the renal hillus: 1.5-2.0mm lateral and 1.5-1.7mm ventral to the surface of the kidney. The injection volume of 500nL per site. Two additional injections per kidney were performed in which the pipette was moved 1.5-2.0 mm toward each pole and using the same depth. These sites were targeted are prior studies in rats indicated the sensory nerves largely innervate the renal pelvis (Marfurt and Echtenkamp 1991). Each kidney within the same mouse received a different WGA-Alexa Fluor tracer. At 5-7 days later, animals were anesthetized with isoflurane and perfused transcardially with 4% paraformaldehyde (in 10mM PBS, pH 7.3). The DRG at T5-L3 and nodose ganglia were harvested,

post-fixed in 4% paraformaldehyde for 1 hr at 4˚C, immersed in 30% sucrose overnight, and sectioned at 20µm using a cryostat. Labeled cells were visualized and quantified using a Leica DM6000b epifluorescence microscope at every other section by 2 independent researchers. To ensure the labeling was dependent on renal nerve transport versus leakage into the bloodstream, the renal tracer injections were performed in an additional set of mice (n=3) after total renal nerve denervation by surgical removal of the renal nerve and 10% phenol application to the renal vessels (see denervation protocol below).

2.3 Experiment 3

Experiment 3 examined the time-course and contribution of the sympathetic nervous system to 2K1C hypertension. Mice were anesthetized with isoflurane (2-3% in 100% oxygen) and instrumented with PA-C10 telemetry units (Data Sciences) advanced 1.5 cm into the femoral artery with the transmitter body secured subcutaneously (sc) in the flank. Mice were treated with Buprenex (0.03 mg/kg, sc, 2x per day for 48 hours) and enrofloxacin (2 mg/kg, sc), returned to home cages, and given 1 week to recover before experiments began. Telemetry data was analyzed beat-to-beat for systolic and diastolic ABP. Mean ABP was calculated by diastolic plus 1/3 pulse pressure. Data were analyzed between 10AM-4PM and 10PM-4AM (lights on 7AM-7PM). After a 7 day recovery and 3 day baseline recording, 2K1C model of hypertension was produced using methods described previously (Warner, Cheng et al. 2012, Kashyap, Boyilla et al. 2016). Mice were anesthetized with isoflurane (2-3% in 100% oxygen). After a retroperitoneal incision, the left kidney was gently retracted. A small section at the midpoint of the renal artery was isolated free from the renal vein and/or renal nerves. A 0.5mm length PTFE tubing (ID: 0.008 x OD: 0.014,

Braintree Scientific SUBL140) was cut longitudinally, placed around the renal artery, and secured by two 10-0 circumferential sutures. In control mice, the left kidney and renal artery were exposed but no clip was implanted. The incisions were closed with suture, and animals treated with Buprenex and enrofloxacin. Ganglionic blockade with hexamethonium (30mg/kg, ip) was performed on Day 0 (before the renal clip surgery), 14, and 21 days relative to 2K1C surgery. On days 22-23, mice were anesthetized with isoflurane (3% in 100% oxygen) and perfused transcardially with saline and 4% paraformaldehyde (in 10mM PBS, pH 7.3). The kidneys were harvested and weighed. A subset of kidneys was embedded in paraffin, sectioned at 3 μm, and counterstained with H&E. The remaining kidneys were processed for immunofluorescence visualization of tyrosine hydroxylase and TRPV1 as described below (Experiment 5).

A second set of 2K1C and sham mice (n=4 per group) without telemetry units were produced to assess renal cytokine expression using qPCR. At 3 weeks after surgery, mice were anesthetized with isoflurane (2-3% in 100% oxygen). The kidneys were harvested, the poles excised, and the middle portion contained the pelvis and cortex was homogenized in TRIzol. RNA was converted to cDNA using a reverse transcription kit (ThermoFisher K1691). Primers were designed using Primar-BLAST (NIH) and purchased from ThermoFisher (see Table 1 for sequences). cDNA, diluted primers, and SYBR Green Master Mix (Bio-Rad 1725121) were combined in a 96 well plate and analyzed in a CFX Connect Real-Time PCR Detection System. Annealing temperature was set to 60°C for all primers and melt curves were generated to assess primer specificity. Gene expression was normalized to B-ACTIN and then quantified using the comparative CT method (ΔΔCT).

Table 1 Primers for qPCR of Kidney Samples

GENE	FWD SEQ	REV SEQ
IL1B	TGCCACCTTTTGACAGTGATG	ATGTGCTGCTGCGAGATTTG
IL2	CAAGCAGGCCACAGAATTGAAA	GGCACTCAAATGTGTTGTCAGA
IL4	ACTTGAGAGAGATCATCGGCA	AGCTCCATGAGAACACTAGAGTT
IL5	AGGCTTCCTGTCCCTACTCAT	CGCCACACTTCTCTTTTTGGC
IL6	CTTGGGACTGATGCTGGTG	TCCACGATTTCCCAGAGAAC
IL10	ACTTTAAGGGTTACTTGGGTTGC	TTCAGCTTCTCACCCAGGGA
IL17F	CGTGAAACAGCCATGGTCAAG	GGGACAGAAATGCCCTGGTT
IL23	ACCAGCGGGACATATGAATCT	AGACCTTGGCGGATCCTTTG
TNFa	TCGTAGCAAACCACCAAGTG	CCTTGAAGAGAACCTGGGAG
MCP1	CCCACTCACCTGCTGCTAC	TTCTTGGGGTCAGCACAGA
COLLAGEN 1	ATCTCCTGGTGCTGATGGAC	ACCTTGTTTGCCAGGTTCAC
FIBRONECTIN	CGAGGTGACAGAGACCACAA	CTGGAGTCAAGCCAGACACA
TGFb	GTGGAAATCAACGGGATCAG	GTTGGTATCCAGGGCTCTCC
IFNg	AGACAATCAGGCCATCAGCAA	TGTGGGTTGTTGACCTCAAACT
B-ACTIN	CAGCTGAGAGGGAAATCGTG	CGTTGCCAATAGTGATGACC

2.4 Experiment 4

Experiment 4 determined whether renal afferent nerve activity differed between kidneys of 2K1C or sham mice. 2K1C and sham mice without telemetry units were produced as described above. At 3 weeks later, mice were anesthetized with isoflurane and instrumented with femoral catheters as described above. Through a retroperitoneal incision, the left and right renal nerves were isolated, placed on a bipolar stainless-steel electrodes, cut proximal, and insulated with KWIK-SIL. Signals were filtered (300-1000 Hz), digitized (2 kHz), full-wave rectified, and integrated (1s time constant) using a Micro1401 and Spike2 software (Cambridge Electronic Design). The raw signal was also analyzed by a window discriminator (FHC) to quantify discharge

rate. The window was set immediately above the estimated noise level and confirmed to produce no events post-mortem. After mice stabilized at 1.8% isoflurane for 20 min, variables were recorded for 20 min. Then, animals were euthanized, noise confirmed for both rectified/integrated signals and the window discriminator using a 5 min average, and the kidneys harvested and weighed.

2.5 Experiment 5

Experiment 5 determined whether total renal nerve denervation or selective afferent renal denervation lowered ABP in 2K1C mice. Mice were implanted with telemetry units as described above. After a 2-week recovery, the left renal artery was isolated and clipped as described above. Immediately prior to clipping, total renal nerve denervation was performed unilaterally to the same kidney by stripping the artery and vein of nerves and connective tissue and painting the vessels with 10% phenol (in 90% ethanol). Selective afferent nerve denervation was performed unilaterally to the same kidney by carefully removing connective tissue overlying the renal artery and vein and painting the vessels with capsaicin (33mM in 5% ethanol/95% saline) for 10 min using a small piece of cotton swab soaked in the capsaicin solution. ABP and heart rate were recorded 3 days before and 21 days after 2K1C surgery. Ganglionic blockade with hexamethonium (30mg/kg, ip) was performed on days 0, 14, 21 relative to 2K1C surgery. On day 22-23, mice were anesthetized with isoflurane and perfused transcardially with 4% paraformaldehyde. Kidneys were harvested, weighed, and sectioned at 10μm using a cryostat. Alternate sections were incubated with polyclonal antibodies for tyrosine hydroxylase (1:2000, EMD Millipore AB152) or TRPV1 (1:500, Alomone Labs ACC-030) overnight at 4˚C with 1% donkey serum (ThermoScientific) and

visualized after with donkey anti-rabbit Alexa Fluor 647 (1:250, Invitrogen, 4˚C overnight incubation). Sections were qualitatively assessed for the presence/absence of immunofluorescent signals by an individual blind to the experimental group. A subset of kidneys from Experiment 1 were included as a positive control.

3.0 Statistical Analysis

All data are presented as mean±SEM plus individual data points when possible. Telemetry, ganglionic blockade, and renal mass were analyzed by a 2-way ANOVA (group and kidney). When significant F values were obtained, independent or paired t-tests with a layered Bonferroni correction was performed to assess group or time differences. The depressor response to ganglionic blockade was calculated by the peak drop (1s) versus baseline (300s) value of mean ABP. qPCR analysis of renal cytokine expression was compared using a 2-way ANOVA (group and kidney) with post hoc testing described above. Responses to stimulation of renal afferents were analyzed by comparing baseline (30s) versus peak (1s) segments. SNA responses during spike-triggered average were compared using a baseline (100ms) versus peak (10ms) segment. Data was analyzed by a 2-way ANOVA (frequency x drug-chlorisondamine-Manning Compound). Renal afferent discharge, rectified and integrated (1s time constant) voltage (signal – noise by nerve crush) and ABP was averaged over a 20 min period and analyzed using a 2-way ANOVA (group and kidney).

4.0 Results

4.1 Experiment 1: Renal Afferent Stimulation in Mice Produces a Sympathetically-Mediated Increase in ABP

Baseline mean ABP and heart rate of mice anesthetized with isoflurane and prepared for recordings were 88±4 mmHg and 603±20 bpm, respectively. Electrical stimulation of the right renal afferent nerve produced frequency-dependent increases in ABP (Figures 1A, B). Heart rate decreased (2Hz: -1±1, 5Hz: -3±1, 10Hz: -18±4*, 20Hz: -19±5*, 30Hz: -17±4*, 50Hz: -24±5* bpm; n=6, *P<0.05 vs baseline). Administration of chlorisondamine decreased baseline ABP from 86±3 to 41±4 mmHg (P<0.01) and largely eliminated these responses (Figures 1A, B). On the other hand, blockade of vasopressin receptors did not significantly alter the pressor response (2Hz: 1±1, 5Hz: 3±1, 10Hz: 5±1, 20Hz: 9±1, 30Hz: 10±2, 50Hz: 10±2 mmHg; n=3, P>0.7 from overall ANOVA).

In a subset of mice (n=4), we performed simultaneous recordings of splanchnic, renal, and lumbar SNA and applied single pulses to the contralateral renal nerve to determine whether activation of renal afferent nerves increases SNA. Figure 1C illustrates the simultaneous SNA recordings and a representative example of the stimulus-triggered averaging of SNA. Stimulation of renal afferents significantly increased contralateral renal, splanchnic, and lumbar SNA with a latency to peak ~100-200 ms (Figure 1D).

A final set of experiments repeated these stimulations in mice anesthetized with urethane. Renal afferent stimulation produced frequency-dependent pressor responses (2Hz: -1±1, 5Hz: 3±1, 10Hz: 7±1, 20Hz: 11±2, 30Hz: 12±3, 50Hz: 12±3 mmHg; n=3) which were also blocked by

chlorisondamine (2Hz: 0±0, 5Hz: 0±0, 10Hz: 1±1, 20Hz: 0±1, 30Hz: 1±1, 50Hz: 2±1 mmHg; n=3). Baseline mean ABP and heart rate in urethane-anesthetized mice was 79±4mmHg and 658±16 bpm, respectively.

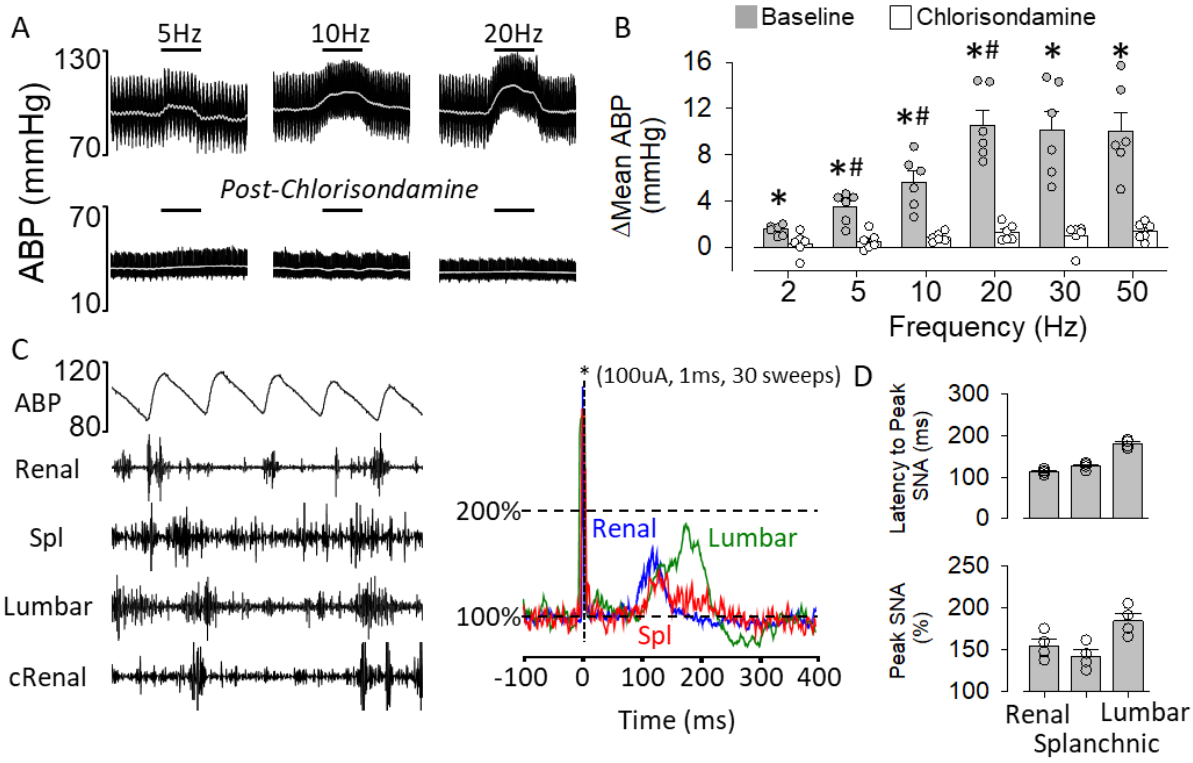

Figure 1 (A) Raw traces of ABP and mean ABP (white) during electrical stimulation of the right renal sensory nerve (1 ms pulse, 200 uA) at 5, 10, and 20 Hz before and after the ganglionic blocker chlorisondamine. **(B)** Mean±SEM and individual data points of the peak change in mean ABP (*P<0.01 vs chlorsidonamine; #P<0.05 vs smaller frequency). **(C)** (LEFT) Simultaneous recording of ABP and renal, splanchnic, lumbar, and contralateral renal SNA in a control mouse. Note pulse-synchronous activity in all 4 sympathetic nerves. (RIGHT) Example of stimulus-triggered averaging during electrical stimulation of the contralateral renal afferent nerve (1 ms, 1 Hz, 100 uA, 30 sweeps) revealed an increase in renal, splanchnic, and lumbar SNA between 100-200 ms. **(D)** Mean±SEM and individual data points of latency to peak (ms) and peak SNA during stimulus-triggered averaging. Baseline nerve activity was normalized to 100%.

4.2 Experiment 2: Location of Renal Sensory Neurons in the Dorsal Root Ganglia

To anatomically map the location of renal sensory neurons in the DRG, mice received an injection of WGA-Alexa Fluor 488 or 594 into the right and left kidney, respectively. Figure 2A illustrates a representative single injection located on the pelvic wall with no tracer deposited in the cortex. Each injection site produced WGA-positive nerve fibers projecting along the pelvic wall. Figure 2A also illustrates examples of labeled cells in the right and left DRG. Figure 2B illustrates the greatest number of labeled cells was located at T11-L1 and T12-L2 for the right and left kidney, respectively. No cells were observed at T5 or T6 levels (data not shown), and few cells were labeled in the contralateral DRG (0.7±0.2 cells per DRG at T11-L2). In addition, the nodose ganglia did not contain labeled cells in 3 of 4 mice (Figure 2B). The only mouse that produced labeling in the nodose ganglia resulted in a few cells on the right side only. Finally, total renal nerve denervation with 10% phenol eliminated the number of labeled cells in the DRG at any level (0±0 cells per DRG at T11-L2, n=3).

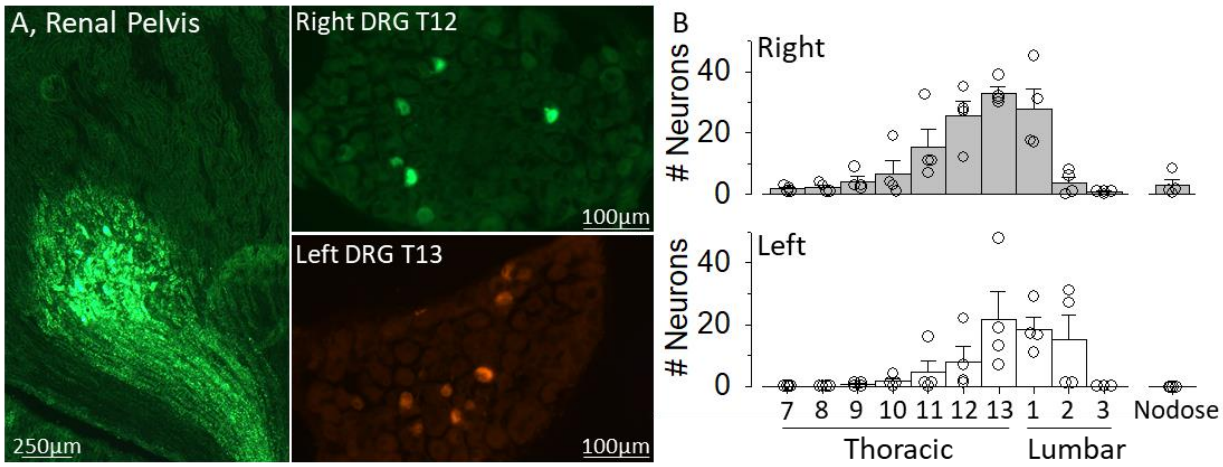

Figure 2 (A) Digital images of a single kidney injection site and labeled DRG neurons. **(B)** Mean±SEM and individual data points for the number of labelled-DRG-neurons per spinal level after injection of WGA-Alexa Fluor 488 or 594

into the right and left kidney, respectively. Total renal nerve denervation eliminated the number of labeled cells in the DRG at any level (0±0 cells per DRG at T11-L2, n=3).

4.3 Experiment 3: 2K1C Hypertension Model in Mice

An initial set of experiments established the 2K1C mouse model of neurogenic hypertension. Unilateral placement of a PTFE clip to model renal stenosis significantly increased mean ABP without changes in heart rate (Figure 3A). These differences were present at day and nighttime periods (data not shown). Ganglionic blockade with hexamethonium produced significantly greater falls in mean ABP at day 14 and 21 versus Day 0 (Figure 3B). Renal mass of 2K1C mice was significantly less in clipped versus unclipped kidneys (Figure 3C). Qualitative analysis of renal histology indicated the presence of damaged glomeruli and renal casts in 2K1C-clipped versus 2K1C-unclipped or sham mice. qPCR analysis of renal samples revealed significant increases in mRNA for various cytokines in 2K1C-clipped versus 2K1C-unclipped or sham kidneys (Table 2).

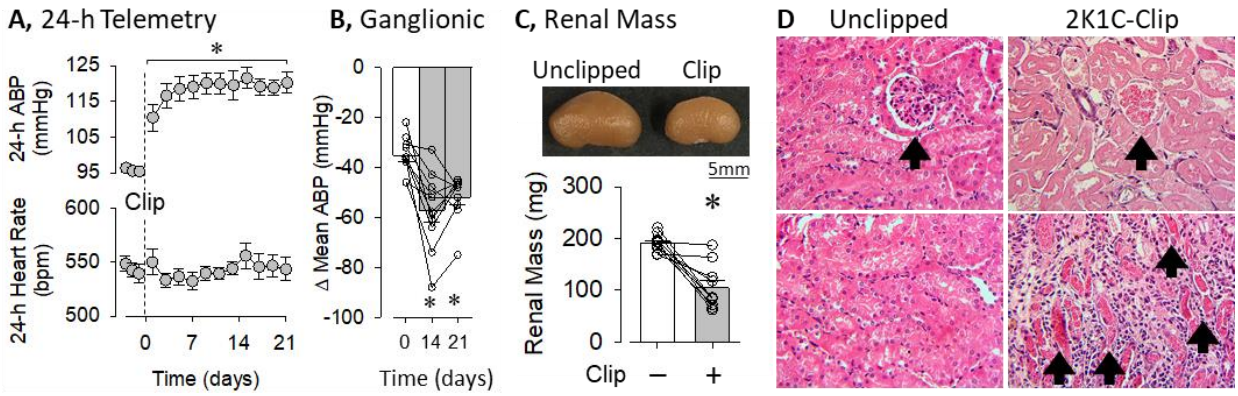

Figure 3 (A) Mean±SEM of 24-h mean ABP and heart rate before and after unilateral clipping of the left renal artery. *P<0.05 versus avg baseline (1-way ANOVA and paired t-tests with layered Bonferonni correction). **(B)** Mean±SEM

and individual data points of changes in mean ABP in response to ganglionic blocker hexamethonium (30mg/kg, ip). *P<0.05 vs Day 0 (paired t-test). **(C)** Images of 2K1C unclipped versus clipped kidneys to illustrate reduction in renal mass after unilateral clipping. Mean±SEM and individual data points of unclipped and clipped kidneys in 2K1C mice. *P<0.05 vs unclipped. **(D)** Renal histology revealed the presence of damaged glomeruli (filled arrow) and renal casts (filled arrow) in clipped but not unclipped kidneys of 2K1C mice.

Table 2 qPCR Analysis of Kidneys from 2K1C and Sham Mice. Values were normalized by B-actin and expressed mean±SEM 2ΔΔCT. Values were statistically analyzed by a 2-way ANOVA (group vs kidney). *P<0.05 unclipped vs clipped kidney in same animal. #P<0.05 right unclipped SHAM kidney vs 2K1C-clipped

	SHAM (n=4)		**2K1C** (n=4)	
Cytokine	**Unclipped-Left**	**Unclipped-Right**	**Clipped-Left**	**Clipped-Right**
IL1b	1.0±0.3	1.1±0.3	1.4±0.3	7.3±2.3 *#
IL2	1.0±0.2	1.1±0.3	1.1±0.5	3.7±0.7 *#
IL5	1.0±0.3	0.8±0.3	1.1±0.3	0.9±0.1
IL6	1.0±0.3	0.4±0.1	0.6±0.1	2.9±0.7 *#
IL10	1.0±0.3	0.4±0.1	0.8±0.1	3.3±0.8 *#
IL17F	1.0±0.1	1.0±0.1	1.3±0.3	0.8±0.3
IL23	1.0±0.1	1.0±0.1	2.3±0.6	1.2±0.1
TNFa	1.0±0.1	0.8±0.1	0.8±0.1	3.4±1.0 *#
MCP1	1.0±0.1	1.0±0.1	1.1±0.1	7.9±2.0 *#
Collagen 1	1.0±0.1	1.1±0.2	1.0±0.1	5.3±1.3 *#
Fibronectin	1.0±0.1	1.0±0.1	1.1±0.1	5.4±1.3 *#
TGFb	1.0±0.1	1.0±0.1	1.2±0.1	2.3±0.3 *#
IFNg	1.0±0.1	1.0±0.1	1.4±0.2	3.6±0.6 *#

4.4 Experiment 4: Renal Afferent Nerve Activity is Elevated in 2K1C Mice

Renal afferent nerve recordings were performed to assess differences in baseline renal sensory nerve activity between 2K1C and sham mice. Baseline mean ABP was significantly

elevated in this group of anesthetized 2K1C versus sham mice (97±3 vs 86±2 mmHg, respectively; P<0.05 t-test). A qualitative assessment of the renal afferent recording suggested the presence of single-units as indicated by the shape and duration of the voltage events. Quantitative analysis revealed that both renal afferent discharge and rectified/integrated voltage was significantly elevated in clipped kidneys of 2K1C mice versus unclipped kidneys of 2K1C or sham mice (Figure 4B). In this cohort, renal mass was significantly lower in 2K1C-clipped versus 2K1C-unclipped or sham kidneys (2K1C-clipped: 68±10 vs 2K1C-unclipped: 181±12 or sham: 182±8 or sham: 171±7 mg, P<0.05 t-tests). A linear regression revealed a significant inverse relationship between renal afferent discharge (r=0.696, P<0.001) or voltage (r=0.688, P<0.001) versus renal mass (plots not shown).

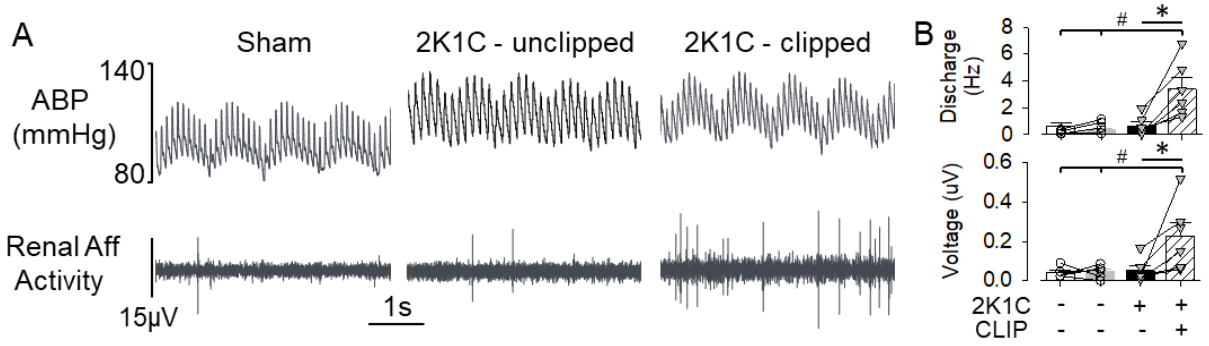

Figure 4 **(A)** Raw traces of ABP, mean ABP (white), and renal afferent nerve activity of a sham, 2K1C-unclipped, and 2K1C-clipped kidneys. **(B)** Mean±SEM and individual data points of renal afferent discharge and full-wave rectified/integrated renal afferent voltage. *P<0.05 2K1C-clipped vs 2K1C-unclipped, #P<0.05 2K1C-clipped vs sham, unpaired 2-tailed t-test

4.5 Experiment 5: Total or Selective Renal Sensory Nerve Denervation Lowers ABP in 2K1C Mice

To determine the contribution of renal efferent versus renal afferent nerves to 2K1C hypertension, ABP telemetry recordings were performed in 2K1C mice with ipsilateral renal denervation or selective ipsilateral renal afferent denervation. Implantation of a renal clip significantly increased mean ABP from baseline levels in sham, ipsilateral renal denervation, and selective renal afferent denervation groups throughout the experimental protocol ($P<0.05$ from overall ANOVAs). However, mean ABP was significantly lower in 2K1C-ipsilateral renal denervation versus 2K1C mice at Days 7-21 (Figure 5). In addition, mean ABP was also significantly lower of 2K1C-capsaicin versus 2K1C mice at Days 1-3 and 11-21 (Figure 5). No significant differences were observed in mean ABP between 2K1C-ipsilateral denervation versus 2K1C-capsaicin. Ganglionic blockade with hexamethonium did not produce a statistically greater depressor response between Day 0, 14, or 21 in 2K1C-ipsilateral renal denervation ($P=0.0967$ from overall 1-way ANOVA) or 2K1C-capsaicin ($P=0.06488$ from overall 1-way ANOVA) groups (Figure 5B). Renal mass was significantly lower in clipped versus unclipped kidneys of 2K1C (105±14 vs 191±5g, respectively; $P<0.01$), 2K1C-ipsilateral denervation (136±16 vs 188±6g, respectively, $P<0.01$), and 2K1C-capsaicin (125±11 vs 184±9g, respectively; $P<0.01$).

Immunofluorescence analysis confirmed the presence of TRPV1- and tyrosine hydroxylase-positive fibers in the kidney of 2K1C mice (Figure 6). However, a qualitative analysis revealed that both markers were absent in mice with ipsilateral renal denervation. Tyrosine hydroxylase, but not TRPV1, fibers were present in mice with selective renal afferent denervation. It is noteworthy that 3 mice in the renal afferent denervation group did display TRPV1 immunofluorescence in the pelvic wall. Consequently, these mice were excluded from the BP data

presented in Figure 5 but had mean ABP values on Day 14 and 21 of 123±5 and 125±4 mmHg, respectively.

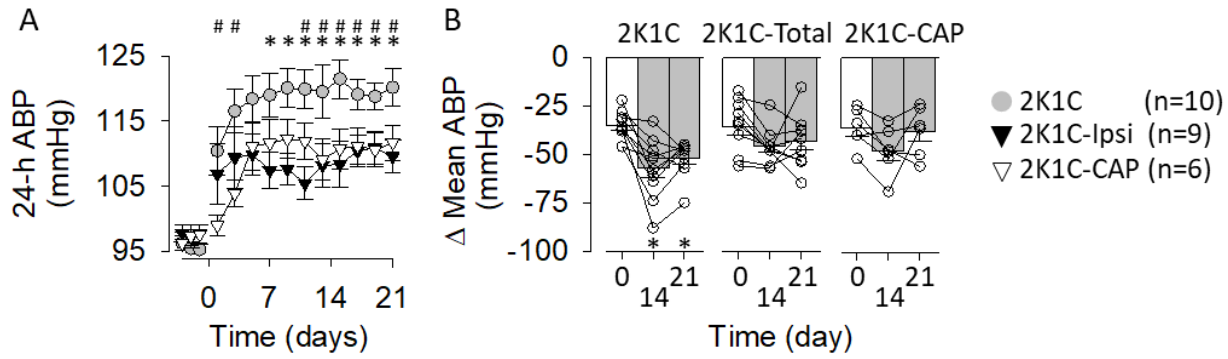

Figure 5 **(A)** Mean±SEM of 24-h mean ABP before and after unilateral clipping of the left renal artery of mice receiving ipsilateral renal denervation or selective afferent renal denervation. Control mice have been replotted from Figure 1. *P<0.05, sham vs ipsilateral renal denervation, #P<0.05, control vs capsaicin (2-way ANOVA followed by t-test with layered Bonferonni correction). **(B)** Mean±SEM and individual data points of changes in mean ABP in response to ganglionic blocker hexamethonium (30mg/kg, ip). *P<0.05 vs Day 0 (paired t-test). Ganglionic blockade with hexamethonium did not produce a greater depressor response between Day 0, 14, or 21 of ipsilateral renal denervation (P=0.0967 from overall 1-way ANOVA) or capsaicin-treated (P=0.06488 from overall 1-way ANOVA) groups. Confirmation of the denervation using immunofluorescence for TRPV1 and tyrosine hydroxylase is presented in Figure 6.

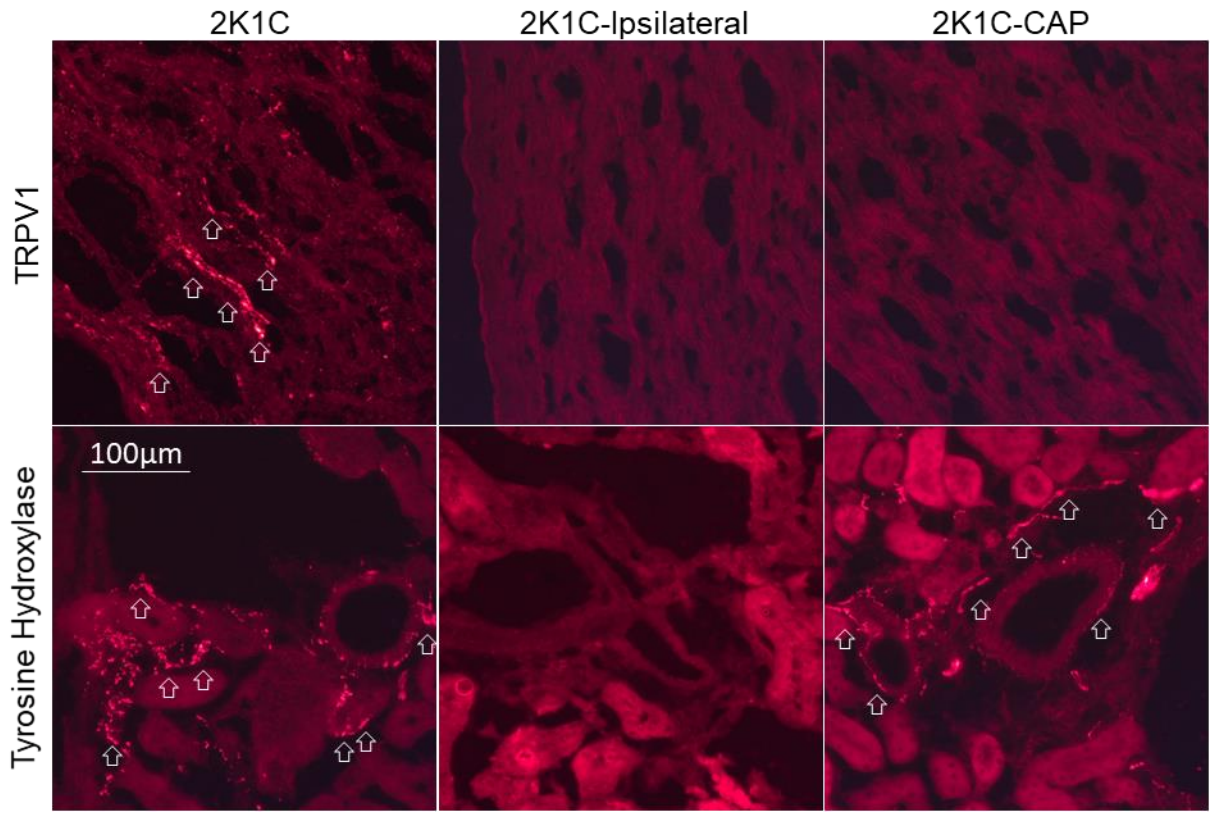

Figure 6 Digital images of immunofluorescence labeling for TRPV1 and tyrosine hydroxylase in clipped kidneys of control, ipsilateral denervated, and capsaicin (renal afferent denervated) mice. Note the presence of TRPV1- versus tyrosine hydroxylase-positive fibers in the kidney of 2K1C sham mice that were predominantly localized to the pelvis versus cortex and medulla, respectively. However, both markers were absent in mice with ipsilateral renal denervation. Tyrosine hydroxylase, but not TRPV1, fibers were present in mice with selective renal afferent denervation. White arrows indicate positive-labeled terminals. Scale bar = 100 µm.

5.0 Discussion

Recent clinical trials and basic research studies underscore the importance of renal afferent nerves in cardiovascular regulation and hypertension (DiBona and Kopp 1997, Krum, Schlaich et al. 2009, Krum, Schlaich et al. 2014, Azizi, Sapoval et al. 2015, Osborn and Foss 2017, Townsend, Mahfoud et al. 2017). Although mice represent the most common biomedical research model currently employed, no information is currently available of mouse renal sensory nerves with respect to the function, anatomical location, and contribution to hypertension. The purpose of this study was to lay the foundational framework and test the contribution of mouse renal sensory nerves to a renal nerve-dependent model of hypertension. For the first time, we have documented that stimulation of these afferent nerves produced a frequency-dependent and sympathetically-mediated increase in ABP. Simultaneous recordings of multiple sympathetic nerves revealed, for the first time, that activation of mouse renal sensory nerves increased splanchnic, lumbar, and renal SNA. Furthermore, the anatomical location of mouse renal sensory cell bodies are distributed in T11-L2 DRG. Next, paired renal afferent nerve recordings provide the first evidence that mouse renal sensory nerve activity is elevated in the 2K1C model of hypertension. Finally, both ipsilateral renal denervation and selective afferent denervation lowered ABP in 2K1C mice. Altogether, these findings provide multiple novel observations in the mouse to suggest that renal afferent nerves become hyperactive to elevate SNA and ABP in 2K1C hypertension.

The majority, if not all, of previous studies to understand the function of renal sensory nerves have been performed in larger animal models (i.e., cats, dogs, and rats). These studies have largely employed supraphysiological stimulation parameters (>30 Hz) and reduced preparations (i.e., barodenervated and vagotomized) to report that renal afferent nerve stimulation increases

ABP and may stimulate vasopressin secretion (Caverson and Ciriello 1987, Caverson and Ciriello 1988, Simon, Kasting et al. 1989). To date, no such data existed in the mouse. The current findings indicate renal afferent stimulation produced frequency-dependent and sympathetically-mediated increases in ABP. First, stimulation frequencies of 5 or 10 Hz increased mean ABP. Although these frequencies are equivalent to the discharge rate of renal afferent nerves in the 2K1C mouse reported herein, single-units were not identified, and the electrical stimulation paradigms may not reflect the patterning of renal afferent discharge. Second, blockade of ganglionic neurotransmission, but not vasopressin receptors, eliminated this pressor response. Next, to determine the extent by which renal afferent activation altered SNA, simultaneous recording of multiple sympathetic nerves revealed an increase in splanchnic, contralateral renal, and lumbar SNA. The latency (~100-200ms) suggests the involvement of supraspinal pathways and likely involves various neuronal populations within the hypothalamus and hindbrain (Caverson and Ciriello 1988, Ammons 1992, Xu, Zheng et al. 2015). The relative contribution of sympathetic efferent nerves innervating the muscle, contralateral kidney, or mesentery to the chronic 2K1C hypertension remains unclear. However, renal denervation of the contralateral or unclipped kidney in 2K1C rats did not affect ABP (Katholi, Whitlow et al. 1982). Altogether, these data provide multiple novel observations in the mouse that renal afferent neurons can elevate ABP through splanchnic, renal, and lumbar SNA.

Renal afferent fibers contain different fiber types including chemo- versus mechanosensitive or myelinated versus unmyelinated (Recordati, Moss et al. 1978, Recordati, Moss et al. 1980, Recordati, Moss et al. 1981, Simon and Schramm 1984, Kopp 2015) that project to the lower thoracic and upper lumbar spinal segments (Ciriello and Calaresu 1983, Donovan, Wyss et al. 1983, Kuo, Nadelhaft et al. 1983). Such data is solely based on studies performed in

rats or larger animal models. The present study documents, for the first time, that injection of neuroanatomical tracers into the mouse renal pelvis labeled renal sensory cell bodies primarily at the T11-L2 DRG. The renal pelvis was targeted since previous studies suggest sensory fibers primarily innervate this region of the kidney (Marfurt and Echtenkamp 1991, Kopp 2015). However, we fully acknowledge that our injections may have missed sensory fibers innervating the renal medulla or cortex and therefore underestimate the number of renal neurons. These findings also highlight that the parasympathetic nervous system does not innervate the mouse kidney. Despite the anatomical location of renal sensory neurons, little is known regarding the neurochemical phenotype and how the neurochemistry corresponds to the properties or response profiles of renal sensory fibers. For example, high concentrations of the TRPV1 agonist capsaicin is used to ablate renal sensory afferents and assumes the majority, if not all, renal sensory neurons express TRPV1. However, the relative expression of TRPV1 (or other common sensory phenotypes) in renal sensory neurons has not been defined for any species. Freisinger (Freisinger, Schatz et al. 2013) reported renal sensory neurons may be distinguished by a tonic versus phasic firing activity and the presence versus absence of Nav1.8 or 1.9 expression. How different neurochemically distinct populations subserve different response profiles or sensory functions to impact cardiovascular function remains unexplored.

A major finding of the present study was renal afferent nerve activity of 2K1C-clipped kidneys was elevated, and denervation of these renal sensory fibers lowered ABP in 2K1C hypertensive mice. These observations extend the original reports that total renal denervation or dorsal rhizotomy lowered ABP in 2K1C or 1-kidney-1-clip rats (Katholi, Whitlow et al. 1982, Katholi, Winternitz et al. 1982, Wyss, Aboukarsh et al. 1986). However, our findings do disagree with a prior study that reported no differences in baseline renal afferent nerve activity between

sham versus 2K1C rats (Kopp and Buckley-Bleiler 1989). Acute insertion of the clip will cause renal ischemia or a reduction in renal perfusion pressure to activate renal sensory nerves, but the mechanism(s) that chronically drive renal afferent activity remain unclear. Removal of the clip at 6 weeks after insertion normalized ABP of 2K1C rats within days, thereby suggesting the renal stenosis provides a chronic stimulus (Katholi, Whitlow et al. 1982). Renal afferent nerves are mechanosensitive (Niijima 1975, Recordati, Moss et al. 1978, Kopp 2015), and structural changes reflected by the reduced renal mass and renal damage may alter the mechanosensitivity and contribute to the disease. Kopp et al (Kopp and Buckley-Bleiler 1989) reported 2K1C hypertensive rats displayed attenuated reno-renal reflexes in both kidneys rather than the stenosed kidney only. Renal afferents are also chemosensitive (Recordati, Moss et al. 1978, Recordati, Moss et al. 1980, Recordati, Moss et al. 1981, Kopp 2015), and the elevated activity in 2K1C-clipped kidneys may reflect changes in the local chemical environment. In this regard, qPCR indicated increased expression of numerous cytokines in the clipped but not unclipped kidneys of 2K1C mice. A subset of these cytokines is also increased in the kidneys of deoxycorticosterone-salt hypertension (Banek, Knuepfer et al. 2016). Cytokines can activate sensory nerves originating in other end-organs (Cook, Christensen et al. 2018, Dong and Dong 2018). Whether renal sensory nerves respond to local cytokines or how the renal sensory innervation of the kidney changes in such disease states remains unknown.

Unilateral renal denervation or selective sensory denervation of the clipped kidney lowered ABP in 2K1C mice. We qualitatively assessed the degree of denervation by the presence or absence of tyrosine hydroxylase or TRPV1 immunoreactivity. Although prior studies have directly assayed renal norepinephrine or CGRP content (Foss, Wainford et al. 2015, Banek, Knuepfer et al. 2016, Foss, Fink et al. 2016, Foss, Fiege et al. 2018), there is not a clearly defined standard or

tissue level for CGRP levels (as for norepinephrine) regarding quantification of a denervated versus partially-denervated kidney. Herein, we were able to discriminate between these two groups by the presence or absence of TRPV1-positive fibers. Indeed, a small cohort of mice (n=3) had residual TRPV1 immunofluorescence and displayed mean ABP values similar to 2K1C animals. Unilateral denervation was performed in the present study at the time of renal artery clipping rather than after hypertension was established. However, prior studies in rats reported that complete unilateral denervation of the clipped kidney but not the contralateral kidney at 6 weeks post-clipping lowered ABP in this model (Katholi, Whitlow et al. 1982, Katholi, Winternitz et al. 1982). Clearly, future studies will need to evaluate the impact of selective afferent denervation after hypertension has been established. Although renal denervation lowered ABP of 2K1C mice in the present study, ABP remained elevated above baseline values (see Figure 5) thereby suggesting additional factors contribute to the hypertension in this model. Such factors likely include renin-angiotensin-aldosterone system activation, renal dysfunction, and vascular dysfunction.

References

Ammons, W. S. (1992). "Bowditch Lecture. Renal afferent inputs to ascending spinal pathways." Am J Physiol **262**(2 Pt 2): R165-176.

Azizi, M., M. Sapoval, P. Gosse, M. Monge, G. Bobrie, P. Delsart, M. Midulla, C. Mounier-Vehier, P. Y. Courand, P. Lantelme, T. Denolle, C. Dourmap-Collas, H. Trillaud, H. Pereira, P. F. Plouin, G. Chatellier and i. Renal Denervation for Hypertension (2015). "Optimum and stepped care standardised antihypertensive treatment with or without renal denervation for resistant hypertension (DENERHTN): a multicentre, open-label, randomised controlled trial." Lancet **385**(9981): 1957-1965.

Banek, C. T., M. M. Knuepfer, J. D. Foss, J. K. Fiege, N. Asirvatham-Jeyaraj, D. Van Helden, Y. Shimizu and J. W. Osborn (2016). "Resting Afferent Renal Nerve Discharge and Renal Inflammation: Elucidating the Role of Afferent and Efferent Renal Nerves in Deoxycorticosterone Acetate Salt Hypertension." Hypertension **68**(6): 1415-1423.

Campese, V. M. and E. Kogosov (1995). "Renal afferent denervation prevents hypertension in rats with chronic renal failure." Hypertension **25**(4 Pt 2): 878-882.

Caverson, M. M. and J. Ciriello (1987). "Effect of stimulation of afferent renal nerves on plasma levels of vasopressin." Am J Physiol **252**(4 Pt 2): R801-807.

Caverson, M. M. and J. Ciriello (1988). "Contribution of paraventricular nucleus to afferent renal nerve pressor response." Am J Physiol **254**(3 Pt 2): R531-543.

Ciriello, J. and F. R. Calaresu (1983). "Central projections of afferent renal fibers in the rat: an anterograde transport study of horseradish peroxidase." J Auton Nerv Syst **8**(3): 273-285.

Cook, A. D., A. D. Christensen, D. Tewari, S. B. McMahon and J. A. Hamilton (2018). "Immune Cytokines and Their Receptors in Inflammatory Pain." Trends Immunol **39**(3): 240-255.

DiBona, G. F. and U. C. Kopp (1997). "Neural control of renal function." Physiol Rev **77**(1): 75-197.

Dong, X. and X. Dong (2018). "Peripheral and Central Mechanisms of Itch." Neuron **98**(3): 482-494.

Donovan, M. K., J. M. Wyss and S. R. Winternitz (1983). "Localization of renal sensory neurons using the fluorescent dye technique." Brain Res **259**(1): 119-122.

Ewen, S., B. Cremers, M. R. Meyer, L. Donazzan, I. Kindermann, C. Ukena, A. G. Helfer, H. H. Maurer, U. Laufs, G. Grassi, M. Bohm and F. Mahfoud (2015). "Blood pressure changes after catheter-based renal denervation are related to reductions in total peripheral resistance." J Hypertens **33**(12): 2519-2525.

Foss, J. D., J. Fiege, Y. Shimizu, J. P. Collister, T. Mayerhofer, L. Wood and J. W. Osborn (2018). "Role of afferent and efferent renal nerves in the development of AngII-salt hypertension in rats." Physiol Rep **6**(3).

Foss, J. D., G. D. Fink and J. W. Osborn (2016). "Differential role of afferent and efferent renal nerves in the maintenance of early- and late-phase Dahl S hypertension." Am J Physiol Regul Integr Comp Physiol **310**(3): R262-267.

Foss, J. D., R. D. Wainford, W. C. Engeland, G. D. Fink and J. W. Osborn (2015). "A novel method of selective ablation of afferent renal nerves by periaxonal application of capsaicin." Am J Physiol Regul Integr Comp Physiol **308**(2): R112-122.

Freisinger, W., J. Schatz, T. Ditting, A. Lampert, S. Heinlein, N. Lale, R. Schmieder and R. Veelken (2013). "Sensory renal innervation: a kidney-specific firing activity due to a unique expression pattern of voltage-gated sodium channels?" Am J Physiol Renal Physiol **304**(5): F491-497.

Grassi, G., G. Seravalle, G. Brambilla, D. Trabattoni, C. Cuspidi, R. Corso, F. Pieruzzi, S. Genovesi, A. Stella, R. Facchetti, D. Spaziani, A. Bartorelli and G. Mancia (2015). "Blood pressure responses to renal denervation precede and are independent of the sympathetic and baroreflex effects." Hypertension **65**(6): 1209-1216.

Hering, D., E. A. Lambert, P. Marusic, A. S. Walton, H. Krum, G. W. Lambert, M. D. Esler and M. P. Schlaich (2013). "Substantial reduction in single sympathetic nerve firing after renal denervation in patients with resistant hypertension." Hypertension **61**(2): 457-464.

Hering, D., P. Marusic, A. S. Walton, E. A. Lambert, H. Krum, K. Narkiewicz, G. W. Lambert, M. D. Esler and M. P. Schlaich (2014). "Sustained sympathetic and blood pressure reduction 1 year after renal denervation in patients with resistant hypertension." Hypertension **64**(1): 118-124.

Kashyap, S., R. Boyilla, P. J. Zaia, R. Ghossan, K. A. Nath, S. C. Textor, L. O. Lerman and J. P. Grande (2016). "Development of renal atrophy in murine 2 kidney 1 clip hypertension is strain independent." Res Vet Sci **107**: 171-177.

Katholi, R. E., P. L. Whitlow, S. R. Winternitz and S. Oparil (1982). "Importance of the renal nerves in established two-kidney, one clip Goldblatt hypertension." Hypertension **4**(3 Pt 2): 166-174.

Katholi, R. E., S. R. Winternitz and S. Oparil (1982). "Decrease in peripheral sympathetic nervous system activity following renal denervation or unclipping in the one-kidney one-clip Goldblatt hypertensive rat." J Clin Invest **69**(1): 55-62.

Kopp, U. C. (2015). "Role of renal sensory nerves in physiological and pathophysiological conditions." Am J Physiol Regul Integr Comp Physiol **308**(2): R79-95.

Kopp, U. C. and R. L. Buckley-Bleiler (1989). "Impaired renorenal reflexes in two-kidney, one clip hypertensive rats." Hypertension **14**(4): 445-452.

Krum, H., M. Schlaich, R. Whitbourn, P. A. Sobotka, J. Sadowski, K. Bartus, B. Kapelak, A. Walton, H. Sievert, S. Thambar, W. T. Abraham and M. Esler (2009). "Catheter-based renal sympathetic denervation for resistant hypertension: a multicentre safety and proof-of-principle cohort study." Lancet **373**(9671): 1275-1281.

Krum, H., M. P. Schlaich, P. A. Sobotka, M. Bohm, F. Mahfoud, K. Rocha-Singh, R. Katholi and M. D. Esler (2014). "Percutaneous renal denervation in patients with treatment-resistant hypertension: final 3-year report of the Symplicity HTN-1 study." Lancet **383**(9917): 622-629.

Kuo, D. C., I. Nadelhaft, T. Hisamitsu and W. C. de Groat (1983). "Segmental distribution and central projections of renal afferent fibers in the cat studied by transganglionic transport of horseradish peroxidase." J Comp Neurol **216**(2): 162-174.

Linz, D., M. Hohl, A. D. Elliott, D. H. Lau, F. Mahfoud, M. D. Esler, P. Sanders and M. Bohm (2018). "Modulation of renal sympathetic innervation: recent insights beyond blood pressure control." Clin Auton Res **28**(4): 375-384.

Mahfoud, F., B. Cremers, J. Janker, B. Link, O. Vonend, C. Ukena, D. Linz, R. Schmieder, L. C. Rump, I. Kindermann, P. A. Sobotka, H. Krum, B. Scheller, M. Schlaich, U. Laufs and M. Bohm

(2012). "Renal hemodynamics and renal function after catheter-based renal sympathetic denervation in patients with resistant hypertension." Hypertension **60**(2): 419-424.

Marfurt, C. F. and S. F. Echtenkamp (1991). "Sensory innervation of the rat kidney and ureter as revealed by the anterograde transport of wheat germ agglutinin-horseradish peroxidase (WGA-HRP) from dorsal root ganglia." J Comp Neurol **311**(3): 389-404.

Niijima, A. (1975). "Observation on the localization of mechanoreceptors in the kidney and afferent nerve fibres in the renal nerves in the rabbit." J Physiol **245**(1): 81-90.

Osborn, J. W. and C. T. Banek (2018). "Catheter-Based Renal Nerve Ablation as a Novel Hypertension Therapy: Lost, and Then Found, in Translation." Hypertension **71**(3): 383-388.

Osborn, J. W. and J. D. Foss (2017). "Renal Nerves and Long-Term Control of Arterial Pressure." Compr Physiol **7**(2): 263-320.

Recordati, G., N. G. Moss, S. Genovesi and P. Rogenes (1981). "Renal chemoreceptors." J Auton Nerv Syst **3**(2-4): 237-251.

Recordati, G. M., N. G. Moss, S. Genovesi and P. R. Rogenes (1980). "Renal receptors in the rat sensitive to chemical alterations of their environment." Circ Res **46**(3): 395-405.

Recordati, G. M., N. G. Moss and L. Waselkov (1978). "Renal chemoreceptors in the rat." Circ Res **43**(4): 534-543.

Simon, J. K., N. W. Kasting and J. Ciriello (1989). "Afferent renal nerve effects on plasma vasopressin and oxytocin in conscious rats." Am J Physiol **256**(6 Pt 2): R1240-1244.

Simon, O. R. and L. P. Schramm (1984). "The spinal course and medullary termination of myelinated renal afferents in the rat." Brain Res **290**(2): 239-247.

Stella, A., R. Golin, I. Busnardo and A. Zanchetti (1984). "Effects of afferent renal nerve stimulation on renal hemodynamic and excretory functions." Am J Physiol **247**(4 Pt 2): H576-583.

Stella, A., L. Weaver, R. Golin, S. Genovesi and A. Zanchetti (1987). "Cardiovascular effects of afferent renal nerve stimulation." Clin Exp Hypertens A **9 Suppl 1**: 97-111.

Townsend, R. R., F. Mahfoud, D. E. Kandzari, K. Kario, S. Pocock, M. A. Weber, S. Ewen, K. Tsioufis, D. Tousoulis, A. S. P. Sharp, A. F. Watkinson, R. E. Schmieder, A. Schmid, J. W. Choi, C. East, A. Walton, I. Hopper, D. L. Cohen, R. Wilensky, D. P. Lee, A. Ma, C. M. Devireddy, J. P. Lea, P. C. Lurz, K. Fengler, J. Davies, N. Chapman, S. A. Cohen, V. DeBruin, M. Fahy, D. E. Jones, M. Rothman, M. Bohm and S. H.-O. M. t. investigators* (2017). "Catheter-based renal denervation in patients with uncontrolled hypertension in the absence of antihypertensive medications (SPYRAL HTN-OFF MED): a randomised, sham-controlled, proof-of-concept trial." Lancet **390**(10108): 2160-2170.

Warner, G. M., J. Cheng, B. E. Knudsen, C. E. Gray, A. Deibel, J. E. Juskewitch, L. O. Lerman, S. C. Textor, K. A. Nath and J. P. Grande (2012). "Genetic deficiency of Smad3 protects the kidneys from atrophy and interstitial fibrosis in 2K1C hypertension." Am J Physiol Renal Physiol **302**(11): F1455-1464.

Witkowski, A., A. Prejbisz, E. Florczak, J. Kadziela, P. Sliwinski, P. Bielen, I. Michalowska, M. Kabat, E. Warchol, M. Januszewicz, K. Narkiewicz, V. K. Somers, P. A. Sobotka and A. Januszewicz (2011). "Effects of renal sympathetic denervation on blood pressure, sleep apnea course, and glycemic control in patients with resistant hypertension and sleep apnea." Hypertension **58**(4): 559-565.

Wyss, J. M., N. Aboukarsh and S. Oparil (1986). "Sensory denervation of the kidney attenuates renovascular hypertension in the rat." Am J Physiol **250**(1 Pt 2): H82-86.

Xiao, L., A. Kirabo, J. Wu, M. A. Saleh, L. Zhu, F. Wang, T. Takahashi, R. Loperena, J. D. Foss, R. L. Mernaugh, W. Chen, J. Roberts, 2nd, J. W. Osborn, H. A. Itani and D. G. Harrison (2015). "Renal Denervation Prevents Immune Cell Activation and Renal Inflammation in Angiotensin II-Induced Hypertension." Circ Res **117**(6): 547-557.

Xu, B., H. Zheng, X. Liu and K. P. Patel (2015). "Activation of afferent renal nerves modulates RVLM-projecting PVN neurons." Am J Physiol Heart Circ Physiol **308**(9): H1103-1111.